

# Anti-inflammatory role of low-intensity pulsed ultrasound in inhibiting lipopolysaccharide-induced M1 polarization of RAW264.7 cells *via* Wnt2b/AXIN/ $\beta$ -catenin

Juan Yin<sup>1,\*</sup>, Yu Bao<sup>2,\*</sup>, Minxin Xu<sup>2</sup>, Ping Li<sup>1</sup>, Zhipeng Zhang<sup>2</sup>, Hui Xue<sup>2</sup> and Xing Yang<sup>3</sup>

<sup>1</sup> Central Laboratory, Suzhou Municipal Hospital, The Affiliated Suzhou Hospital of Nanjing Medical University, Gusu School, Nanjing Medical University, Suzhou, China

<sup>2</sup> Department of Stomatology, Suzhou Municipal Hospital, The Affiliated Suzhou Hospital of Nanjing Medical University, Gusu School, Nanjing Medical University, Suzhou, China

<sup>3</sup> Department of Orthopedics, Suzhou Municipal Hospital, The Affiliated Suzhou Hospital of Nanjing Medical University, Gusu School, Nanjing Medical University, Suzhou, China

\* These authors contributed equally to this work.

## ABSTRACT

**Background:** Low-intensity pulsed ultrasound (LIPUS) is a special type of low-intensity ultrasound. In periodontal disease, LIPUS is applied as an adjuvant and non-invasive treatment. It has been reported that LIPUS significantly shifts the macrophage phenotype from M1 to M2, but the specific mechanism behind this shift is still unknown.

**Methods:** RAW264.7 cells were induced to M1/M2 polarization with lipopolysaccharide (LPS)/interleukin-4 (IL4). LIPUS was performed for 25 min two times, 24 h apart, at an intensity of 45 mW/cm<sup>2</sup> to stimulate RAW264.7 cells. PolyA mRNA sequencing was conducted of both the LPS-induced RAW264.7 cells and the LPS-induced RAW264.7 cells with LIPUS treatment. The expression of Wnt2b in RAW264.7 cells was downregulated by siRNA. The macrophage surface markers and downstream inflammatory cytokines were detected using flow cytometry. The relative expression of proteins in the Wnt2b/AXIN/ $\beta$ -catenin pathway was assessed using reverse transcription real-time polymerase chain reaction (RT-qPCR) and Western blot.

**Results:** LIPUS reversed the M1 polarization of RAW264.7 cells, with decreased expression of CD80 and CD86. In addition, LIPUS enhanced the M2 polarization of RAW264.7 cells, with upregulated expression of CD163 and CD206. The polyA mRNA sequencing results indicated that the Wnt signaling pathway participated in the M1 polarization of LIPUS-treated RAW264.7. The results of the RT-qPCR showed a higher expression of Wnt2b in LIPUS-treated and M1- or M2-polarized RAW264.7 cells. Knocking down Wnt2b was shown to reverse the inhibitory effect of LIPUS on M1 polarization and increase the expression of CD80 and CD86. Wnt2b knockdown also regulated downstream AXIN,  $\beta$ -catenin, and inflammatory factors such as tumor necrosis factor alpha (TNF $\alpha$ ) and interleukin-6 (IL6).

Submitted 31 May 2024  
Accepted 14 October 2024  
Published 13 November 2024

Corresponding authors  
Hui Xue, xuehuislyy@126.com  
Xing Yang, xingyangsz@126.com

Academic editor  
Santosh Patnaik

Additional Information and  
Declarations can be found on  
page 17

DOI 10.7717/peerj.18448

© Copyright  
2024 Yin et al.

Distributed under  
Creative Commons CC-BY 4.0

OPEN ACCESS

**Conclusions:** LIPUS plays an anti-inflammatory role by inhibiting LPS-induced M1 polarization of RAW264.7 cells in a Wnt2b/AXIN/ $\beta$ -catenin-dependent way. LIPUS may play a therapeutic role in periodontal diseases by inhibiting inflammation through the regulation of macrophage differentiation.

**Subjects** Cell Biology, Dentistry

**Keywords** Low-intensity pulsed ultrasound, Anti-inflammatory, M1 polarization, WNT2b, Periodontal disease

## INTRODUCTION

Periodontal disease is a chronic inflammatory gum disease that increases in prevalence with age, afflicting about 10% of the adult population (*Bertolini & Clark, 2024; Hajishengallis, 2022*). In severe cases, periodontal disease can result in tooth loss. Periodontal disease is associated with cytokine dysregulation, including increased pro-inflammatory cytokines and decreased anti-inflammatory cytokines (*Pamuk & Kantarci, 2022*). Macrophages respond early to tissue injury in periodontal disease, and an increased ratio of pro-inflammatory phenotypes over anti-inflammatory phenotypes of macrophages in the tissue has been associated with disease severity (*Zhou et al., 2019*). Physical therapy plays an important role in the treatment of periodontal disease.

Low-intensity pulsed ultrasound (LIPUS) is a special type of low-intensity ultrasound. LIPUS outputs pulsed waves with an intensity of less than  $1 \text{ W/cm}^2$  and a frequency of 1 to 3 MHz (*Palanisamy et al., 2022*). LIPUS is different from the ultrasounds applied in diagnostic imaging, which have intensities ranging from  $0.05\text{--}0.5 \text{ W/cm}^2$ , and ultrasounds in surgery, which have high intensities around  $0.2\text{--}100 \text{ W/cm}^2$  but can go up to  $10,000 \text{ W/cm}^2$  (*Jiang et al., 2019*). For therapeutic applications, LIPUS provides non-invasive physical stimulation while transmitting acoustic energy to the injured tissue in low-intensity and pulsed output mode (*Jiang et al., 2019; Li et al., 2023*).

LIPUS has been used for decades as therapy for various diseases, including bone healing, soft-tissue regeneration, inflammation inhibition, neuromodulation, and dental treatment (*Jiang et al., 2019; Seasons et al., 2024; Wu et al., 2024*). LIPUS stimulation on bone marrow-derived mesenchymal stem cells (BMSCs) has been shown to significantly increase the secretion of extracellular vesicles (EVs). Moreover, EVs generated from LIPUS-treated BMSCs possess much stronger anti-inflammatory functionality than EVs generated without LIPUS stimulation (*Li et al., 2023*). In periodontal disease, LIPUS is generally applied as an adjuvant and non-invasive treatment. Previous studies have shown that LIPUS promotes the formation and migration of periodontal ligament stem cell sheets and ectopic periodontal tissue regeneration (*Li et al., 2021a; Wang et al., 2018a, 2022*). The cell-derived factor-1 (SDF1)/C-X-C motif chemokine receptor 4 (CXCR4) signaling pathway is involved in the LIPUS-promoted periodontal ligament stem cell migration (*Wang et al., 2018a*). LIPUS can also alleviate endoplasmic reticulum stress and inflammation while increasing the bone formation capacity of periodontal ligament stem cells derived from patients with periodontitis (*Li et al., 2020a*). Autophagy is activated by

LIPUS in periodontal ligament cells (Li et al., 2020b). The present study explored the specific mechanisms of LIPUS treatment in periodontal disease.

The Wnt/ $\beta$ -catenin pathway plays critical roles in embryonic development and adult tissue homeostasis. The Wnt pathway depends on the nuclear translocation of  $\beta$ -catenin and the activation of target genes via T cell factor 1 (TCF)/lymphoid enhancer factor (LEF) transcription factors. Once activated, Wnt/ $\beta$ -catenin facilitates the expression of genes involved in cell proliferation, survival, differentiation, and migration (Liu et al., 2022). Wnt/ $\beta$ -catenin is also involved in periodontitis (Bao et al., 2021). In a mouse model, the inhibition of the Wnt/ $\beta$ -catenin signaling pathway by IWR-1 (a small molecule inhibitor for Wnt signaling) promoted the spread of periapical lesions, resulting in suppressed expression levels of *Runx2* and *Col1a1*, which are markers of osteoblast differentiation (Naruse et al., 2021). Activation of the Wnt/ $\beta$ -catenin signaling pathway reduced the periapical lesion volume and accelerated the spread of *Runx2* and *Col1a1* (Naruse et al., 2021). A separate study found that the crosstalk between Wnt3a/ $\beta$ -catenin and NF- $\kappa$ B signaling contributes to apical periodontitis (Guan et al., 2021), but there are no reports of Wnt2b's possible role in periodontitis.

Wnt signaling could modulate macrophage polarization, the key regulator in inflammation and healing (Abaricia et al., 2020; Wu et al., 2023). A previous study found Wnt signaling enhanced the response of macrophages to interleukin-4 (IL4), which promoted the resolution of atherosclerosis (Weinstock et al., 2021). The activation of Wnt/ $\beta$ -catenin signaling facilitates M2 macrophage polarization (Jiang et al., 2021; Tian et al., 2020). Another study found the expressions of Wnt2b and Wnt5a were highly associated with tumor-associated M2 macrophages in non-small cell lung cancer (Sumitomo et al., 2022). Modulating macrophage polarization may be a beneficial target in the treatment of periodontitis.

The present study hypothesizes that LIPUS could regulate the Wnt signaling to modulate the polarization of macrophages. A recently published study reported that LIPUS (60 mW/cm<sup>2</sup>) significantly shifted the macrophage phenotype from M1 to M2, which promoted the regeneration of skeletal muscle with higher expression of Frizzled 5 (FZD5) and  $\beta$ -catenin (Qin et al., 2023). Therefore, LIPUS may regulate Wnt2b, another important protein in Wnt signaling. This study focuses on the role and mechanism of LIPUS in inhibiting lipopolysaccharide (LPS)-induced M1 polarization of RAW264.7 cells. This study aims to discover the specific mechanism of LIPUS in the polarization of macrophages and the treatment of periodontal disease.

## MATERIALS AND METHODS

### M1/M2 polarization of RAW264.7 cells

RAW264.7 cells (CL-0190; Procell, Wuhan, China) were cultured with DMEM (SH30243.01; Hyclone, Logan, UT, USA) containing 10% FBS (10270-106; Gibco, Carlsbad, CA, USA), and inoculated with  $1.5 \times 10^6$  cells/mL. For the cell culture, all operating steps were performed as outlined in the Cell Culture Basics Handbook (Thermo Fisher Scientific, Waltham, MA, USA). M1 polarization of RAW264.7 cells was induced by

100 ng/mL Lipopolysaccharides (LPS, HY-D1056; MCE, Monmouth Junction, NJ, USA) for 48 h. M2 polarization of RAW264.7 cells was induced by 10 ng/mL IL4 (CK15; NoVo protein, Shanghai, China) for 48 h.

### Treatment of cells with low-intensity pulsed ultrasound

The macrophages were treated with a low-intensity pulsed ultrasound therapy instrument (OSTEOTRON IV; ITO, Tokyo, Japan) at an intensity of 45 mW/cm<sup>2</sup>. Each group of cells was treated twice for 25 min each, with a 24-h interval between treatments (*Liang et al., 2020; Majnooni et al., 2022; Wang et al., 2018b*).

### PolyA mRNA sequencing

The polyA mRNA sequencing of LPS-induced RAW264.7 cells and LPS-induced RAW264.7 cells treated with LIPUS was conducted at Ribobio Co. Ltd (Guangzhou, China). Total RNA was isolated from RAW264.7 cells using the Magzol Reagent (Magen, Guangdong, China). The mRNA was enriched by oligodT using NEBNext® Poly(A) mRNA Magnetic Isolation Module (NEB, Ipswich, MA, USA) and then the mRNA was fragmented to approximately 200 bp. The cDNA was synthesized using the NEBNext® Ultra™ RNA Library Prep Kit for Illumina. The libraries were sequenced by Illumina (Illumina, San Diego, CA, USA) with 150 bp paired ends at Ribobio Co., Ltd. (Ribobio, Guangzhou, China). Differential expression was assessed by DESeq/DESeq2/edgeR/DEGseq using read counts as input. Differentially expressed genes were considered those with fold change >2 and adjusted *P*-value < 0.05. The heat map analysis and KEGG ontology enrichment analysis were based on the differentially expressed genes. For the KEGG enrichment analysis, *P*-value < 0.05 was considered as significant enrichment of the gene sets.

### SiRNA of Wnt2b

The expression of Wnt2b in RAW264.7 cells was downregulated by siRNA (Ribobio, Guangzhou, China). The siRNA sequences were as follows: siRNA1 sense, GGACUGA UCUUGUCUACUUTT; siRNA1 antisense, AAGUAGACAAGAUCAGUCCTT; siRNA2 sense, GUAGUGACAACAUCUUAUATT; siRNA2 antisense, UAAUGGAUGUUGUCA CUACTT; siRNA3 sense, CGAGUGAUCUGUGACAACATT; and siRNA3 antisense, UGUUGUCACAGAUCACUCGTT. RAW264.7 cells were seeded in a 10 cm cell culture dish at a density of  $1.5 \times 10^6$  cells/mL. Then, 120  $\mu$ L  $1 \times$  riboFECT™ CP buffer (Ribobio, Guangzhou, China), 10  $\mu$ L siRNA (20  $\mu$ M), and 12  $\mu$ L riboFECT™ CP reagent (Ribobio, Guangzhou, China) were mixed at room temperature for 15 min. The mixture was then added to the RAW264.7 cells in 2 mL DMEM with 10% FBS for a final concentration of 100 nM siRNA. Then, the RAW264.7 cells were cultured at 5% CO<sub>2</sub> and 37 °C for 48 h. Cell culture supernatant was collected for detecting the inflammatory cytokines by flow cytometry. Cells were harvested for detecting macrophage surface markers by flow cytometry and proteins of the Wnt signaling pathway by western blot.

**Table 1 Primers for qPCR.**

Items	Sequences (5'-3')
$\beta$ -actin Forward	GCAGGAGTACGATGAGTCCG
$\beta$ -actin Reverse	ACGCAGCTCAGTAACAGTCC
Wnt 2b Forward	ACTGGGGTGGCTGTAGTGAC
Wnt 2b Reverse	ACCACAGCGGTTGTTGTGTA
CD80 Forward	GGAGATGCTCACGTGTCAGA
CD80 Reverse	CAACGATGACGACGACTGTT
CD86 Forward	TCAGTGATCGCCAACTTCAG
CD86 Reverse	TTAGGTTTCGGGTGACCTTG
CD163 Forward	TGGTGTGCAGGGAATTACAA
CD163 Reverse	CGCCACTGAGCATAGTGAAA
CD206 Forward	CAAGGAAGGTTGGCATTGT
CD206 Reverse	CCTTTCAGTCCTTTGCAAGC

### Detecting the relative expression of macrophage surface markers and proteins in the Wnt2b/AXIN/ $\beta$ -catenin pathway by reverse transcription real-time polymerase chain reaction and Western blot

The relative expression of macrophage surface markers and proteins in the Wnt2b/AXIN/ $\beta$ -catenin pathway was detected by reverse transcription real-time polymerase chain reaction (RT-qPCR). RNA was isolated using the TRIZOL (15596026; Invitrogen, Waltham, MA, USA) reagent, according to the manufacturer's instructions. The concentration and quality of isolated RNA were detected using a NanoDrop Lite (Thermo, Waltham, MA, USA). The RNA was reverse-transcribed into cDNA using a PrimeScript™ Master Mix-Perfect Real-Time kit (TKR-RR036A; Takara, Kusatsu, Shiga, Japan). A Premix qPCR quantitative kit TB Green® Premix Ex Taq™ II-Tli RNaseH Plus (TKR-RR820B A  $\times$  2, Takara, Shiga, Japan) was used to detect the transcription levels of Wnt2b, with  $\beta$ -actin as the reference gene. The primer sequences used in this study are shown in Table 1.

Western blot was used to detect the relative expression of Wnt2b, AXIN, and  $\beta$ -catenin, with GAPDH as the reference protein. Western blot was performed using the methods outlined in our previous study (Yin *et al.*, 2020) and the procedures outlined in Western blotting protocols (BioRad, Hercules, CA, USA). Primary antibodies used in the study included Wnt2b (66656-1-Ig; Proteintech, CA, Rosemont, IL, USA), AXIN (20540-1-AP; Proteintech, Rosemont, Illinois, China),  $\beta$ -catenin (51067-2-AP; Proteintech, Rosemont, IL, USA), and GAPDH (10494-1-AP; Proteintech, Rosemont, IL, USA).

### Detecting the macrophage surface markers with flow cytometry

The surface markers of M1/M2 polarization were detected by flow cytometry. For M1 polarization, CD80 and CD86 were detected using the fluorescently labeled PE Anti-CD80 antibody (104707; Biolegend, San Diego, CA, USA) and Pacific Blue Anti-CD86 antibody

(105021; Biolegend, San Diego, CA, USA). For M2 polarization, CD206 and CD163 were detected using the fluorescently labeled APC Anti-CD206 antibody (141707; Biolegend, San Diego, CA, USA) and PE Anti-CD163 antibody (111803; Biolegend, San Diego, CA, USA). Methods for flow cytometry detection followed the standard operation of the BD Canto II (BD, Franklin Lakes, NJ, USA).

### **Detecting the inflammatory cytokines of the cell culture supernatant with flow cytometry**

The inflammatory cytokines of the cell culture supernatant were detected by flow cytometry using the BD™ Cytometric Bead Array (CBA) Mouse Th1/Th2/Th17 CBA Kit (560485; BD, Franklin Lakes, NJ, USA), according to the manufacturer's instructions. The concentration of interleukin-2 (IL2), IL4, interleukin-6 (IL6), interleukin-10 (IL10), tumor necrosis factor alpha (TNF $\alpha$ ), intracellular interferon gamma (INF $\gamma$ ), and interleukin-17A (IL17A) was detected.

### **Statistical analysis**

Statistical analysis in this study was performed using GraphPad Prism 8.0.1 (GraphPad Software, San Diego, CA, USA). One-way ANOVA analysis of variance was performed using repeated measurements. If the variance was homogeneous, the Dunnett method was used to compare the difference between the experimental group and the control group. If the variances were not homogeneous, Dunnett's T3 method was used to compare the differences between the groups. The results are shown as the mean  $\pm$  SD.  $P < 0.05$  was considered as statistically significant.

## **RESULTS**

### **Low-intensity pulsed ultrasound inhibited the M1 polarization of RAW264.7 cells with downregulation of CD80 and CD86**

To study the role of LIPUS on M1 polarization, the RAW264.7 cells were induced to M1 polarization using LPS. The expression of CD80 and CD86, which are biomarkers of M1 polarization, was detected using flow cytometry and RT-qPCR. The results of flow cytometry showed that the expression of CD80 (Fig. 1A) and CD86 (Fig. 1B) was enhanced in RAW264.7 cells induced by LPS, which indicated M1 polarization. While LIPUS reversed the upregulation effect of LPS on the expression of CD80 (LPS =  $1,512 \pm 36.57$ ; LPS + LIPUS =  $1,049 \pm 4.51$ ; Fig. 1A) and CD86 (LPS =  $544.01 \pm 100.60$ ; LPS + LIPUS =  $373.70 \pm 8.15$ ; Fig. 1B). The relative expression of CD80 and CD86 detected using RT-qPCR were consistent with those of flow cytometry (Fig. 1C). These results show that LIPUS inhibited M1 polarization.

### **Low-intensity pulsed ultrasound promoted the M2 polarization of RAW264.7 cells with upregulation of CD163 and CD206**

To study the roles of LIPUS on M2 polarization, the RAW264.7 cells were induced to M2 polarization using IL4. The expression of CD163 and CD206, which are biomarkers of M1

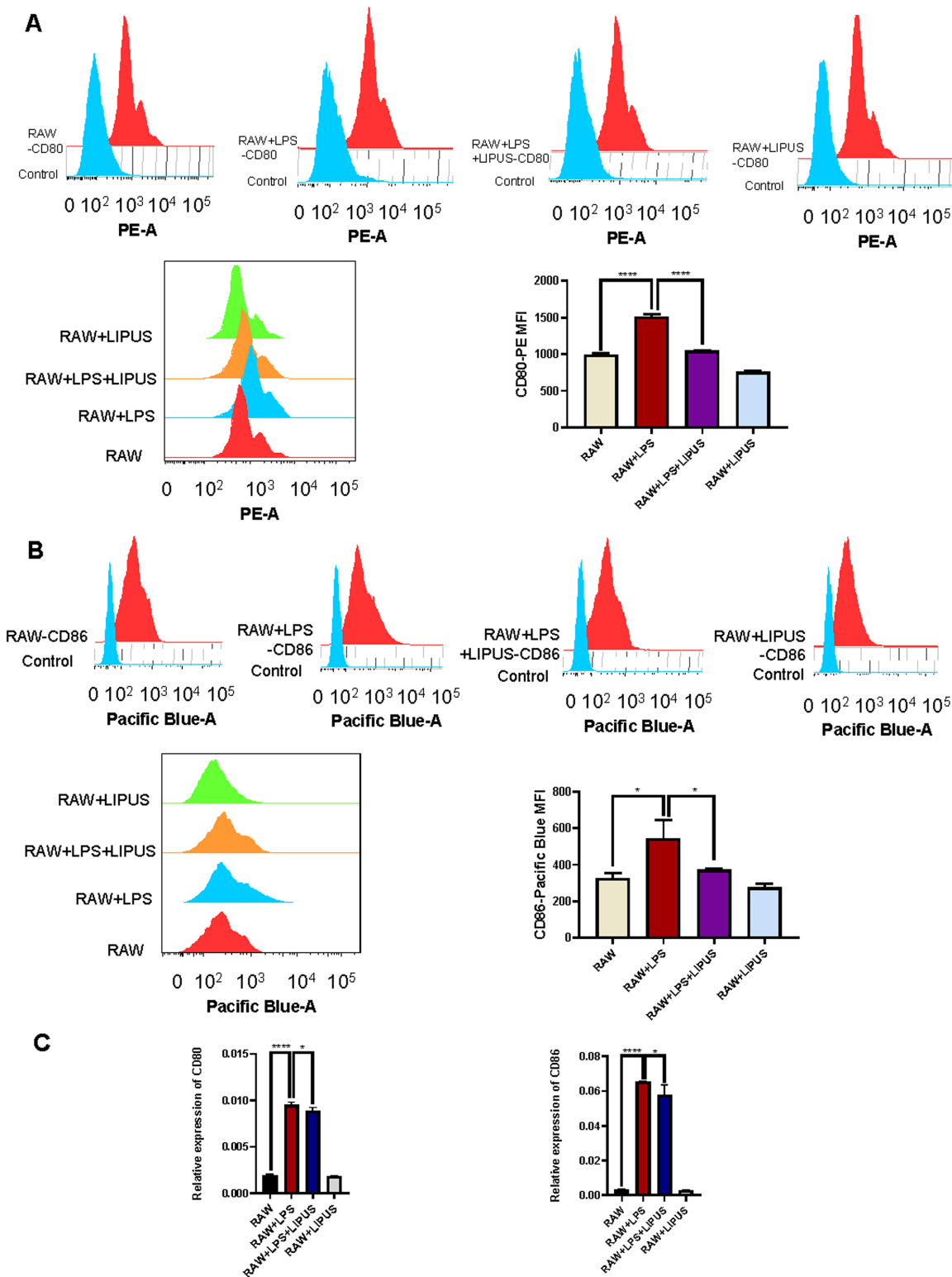


**Figure 1** Low-intensity pulsed ultrasound inhibited the M1 polarization of RAW264.7 cells. (A) Expression of CD80 was detected by flow cytometry. (B) Expression of CD86 was detected by flow cytometry. (C) Relative expression of CD80 and CD86 referring to  $\beta$ -actin detected by RT-qPCR. RAW indicates RAW264.7 cells used as control. RAW + LPS indicates RAW264.7 cells treated with 100 ng/mL LPS to induce macrophage-like M1 polarization. RAW + LPS + LIPUS indicates RAW264.7 cells treated with 100 ng/mL LPS and low-intensity pulsed ultrasound. RAW + LIPUS indicates RAW264.7 cells treated with low-intensity pulsed ultrasound. \* $P < 0.05$ , \*\*\*\* $P < 0.0001$ . [Full-size !\[\]\(fd7fe780e8fd8eece60268c87d0c3e04\_img.jpg\) DOI: 10.7717/peerj.18448/fig-1](https://doi.org/10.7717/peerj.18448/fig-1)

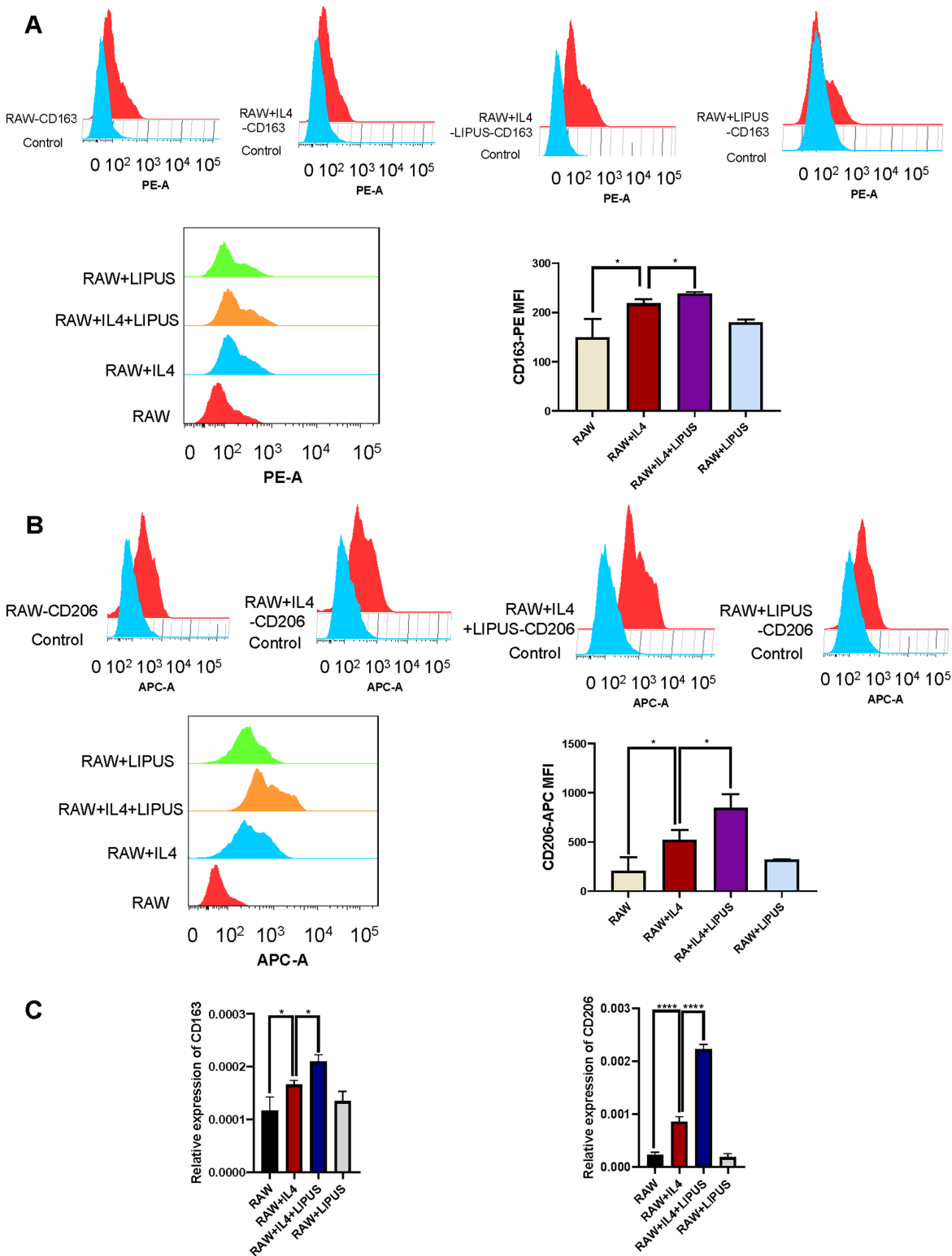


**Figure 2** Low-intensity pulsed ultrasound promoted the M2 polarization of RAW264.7 cells. (A) Expression of CD163 was detected by flow cytometry. (B) Expression of CD206 was detected by flow cytometry. (C) Relative expression of CD163 and CD206 referring to  $\beta$ -actin detected by RT-qPCR. RAW indicates RAW264.7 cells used as control. RAW+IL4 indicates RAW264.7 cells treated with 20 ng/mL IL4 to induce macrophage-like M2 polarization. RAW+IL4+LIPUS indicates RAW264.7 cells treated with 20 ng/mL LIPUS and low-intensity pulsed ultrasound. RAW+LIPUS indicates RAW264.7 cells treated with low-intensity pulsed ultrasound. \* $p < 0.05$ , \*\*\*\* $p < 0.0001$ . Full-size [DOI: 10.7717/peerj.18448/fig-2](https://doi.org/10.7717/peerj.18448/fig-2)



polarization, were detected using flow cytometry and RT-qPCR. The expression of CD163 (Fig. 2A) and CD206 (Fig. 2B) was enhanced in RAW264.7 cells by IL4 induction, while LIPUS promoted the expression of CD163 (IL4 =  $218.30 \pm 8.74$ ; IL4 + LIPUS =  $238.30 \pm 3.22$ ; Fig. 2A) and CD206 (IL4 =  $524.70 \pm 95.69$ ; IL4 + LIPUS =  $847.00 \pm 140.80$ ; Fig. 2B). The relative expression of CD163 and CD206 detected using RT-qPCR were consistent with those of flow cytometry (Fig. 2C). These results indicated that LIPUS promoted M2 polarization.

### **Wnt signaling pathway participated in the inhibition of M1 polarization of RAW264.7 cells by low-intensity pulsed ultrasound**

To discover the target gene of RAW264.7 cells, polyA mRNA was sequenced of both RAW264.7 cells induced by LPS and LPS-induced RAW264.7 cells treated with LIPUS. The sequencing results showed that there were 335 upregulated and 288 downregulated genes (Figs. 3A, 3B). The principal component analysis (PCA) indicated that the six samples were split into two groups: LPS and LPS + LIPUS (Fig. 3C). Gene Ontology (GO) and Kyoto Encyclopedia of Genes and Genomes (KEGG) pathway analyses indicated that the Wnt signaling pathway and HIPPO signaling pathway participated in the inhibition of M1 polarization of RAW264.7 cells by low-intensity pulsed ultrasound (Figs. 3D, 3E). Wnt2b was significantly upregulated in the LPS-induced RAW264.7 cells with LIPUS treatment compared with the LPS-induced RAW264.7 cells.

### **Low-intensity pulsed ultrasound promoted the relative expression of Wnt2b**

To verify the results of polyA mRNA sequencing, RT-qPCR was used to detect the relative expression of Wnt2b, one of the key proteins in the Wnt signaling pathway (Fig. 4). LIPUS promoted the relative expression of Wnt2b in the M1-polarized RAW264.7 cells (LPS =  $0.21 \pm 0.02$ ; LPS + LIPUS =  $0.86 \pm 0.10$ ) and in the M2-polarized RAW264.7 cells (IL4 =  $7.73 \pm 0.19$ ; IL4 + LIPUS =  $8.40 \pm 0.31$ ). These results were in line with the results of the polyA mRNA sequencing.

### **Knocking down Wnt2b could reverse the inhibitory effect of low-intensity pulsed ultrasound on the M1 polarization of RAW264.7 cells**

To study the function of Wnt2b in the M1 polarization of RAW264.7 cells with LIPUS treatment, the expression of Wnt2b was knocked down by siRNA. The expression of CD80 (LPS + LIPUS + Wnt2bsiNC =  $163.70 \pm 1.53$ ; LPS + LIPUS + Wnt2bsi1 =  $225.70 \pm 5.69$ ; LPS + LIPUS + Wnt2bsi2 =  $214.30 \pm 2.08$ ; LPS + LIPUS + Wnt2bsi3 =  $226.30 \pm 3.22$ , Fig. 5A) and CD86 (LPS + LIPUS + Wnt2bsiNC =  $203.30 \pm 4.93$ ; LPS + LIPUS + Wnt2bsi1 =  $365.30 \pm 20.03$ ; LPS + LIPUS + Wnt2bsi2 =  $384.00 \pm 14.00$ ; LPS + LIPUS + Wnt2bsi3 =  $363.00 \pm 8.00$ , Fig. 5B) could be reversed in the LPS-induced RAW264.7 cells with the treatment of Wnt2b siRNAs and LIPUS. Knocking down Wnt2b increased the expression of CD80 and CD86, which indicated that the inhibitory effect of LIPUS on the M1 polarization of RAW264.7 cells is dependent on Wnt2b.

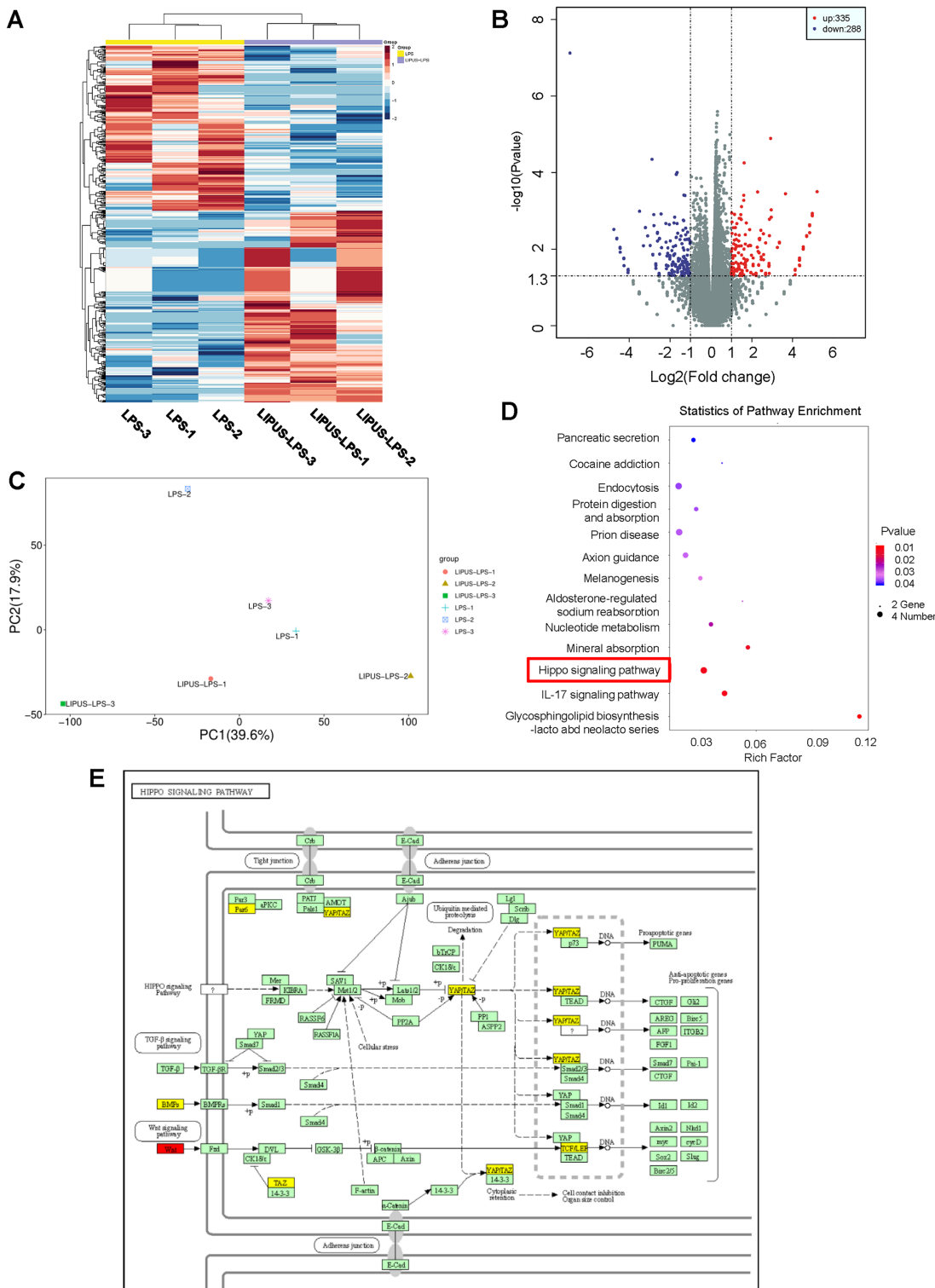


**Figure 3** PolyA mRNA sequencing results of LPS-induced RAW264.7 cells and LPS-induced RAW264.7 cells treated with low-intensity pulsed ultrasound. (A) Heatmap and (B) Volcano plot of the sequencing results show that there were 335 upregulated and 288 downregulated genes. (C) Principal component analysis (PCA) indicated that the six samples were split into two groups: LPS and LIPUS-LPS. (D) GO and (E) KEGG pathway analyses indicated that the Wnt signaling pathway and HIPPO signaling pathway participated in the inhibition of M1 polarization of RAW264.7 cells by low-intensity pulsed ultrasound. LPS indicates RAW264.7 cells treated with 100 ng/mL LPS. LIPUS-LPS indicates RAW264.7 cells treated with 100 ng/mL LPS and low-intensity pulsed ultrasound.

Full-size DOI: 10.7717/peerj.18448/fig-3

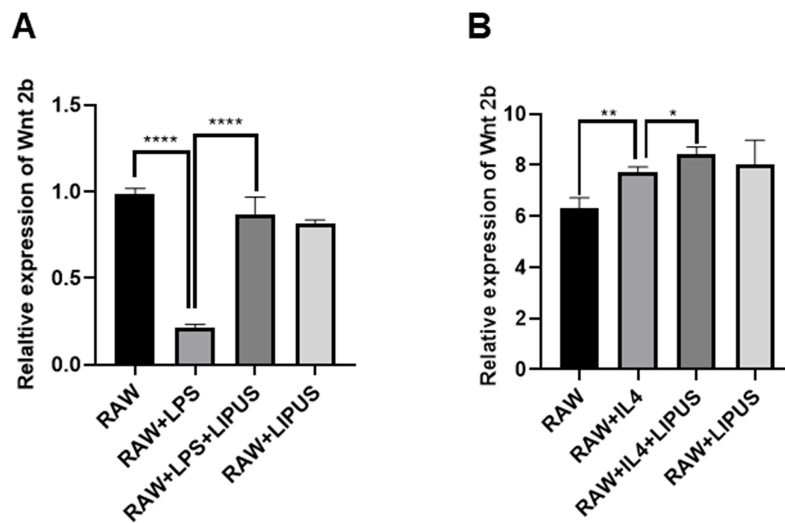


**Figure 4** Low-intensity pulsed ultrasound promoted the relative expression of Wnt2b. The relative expression of Wnt2b, one of the key proteins in the Wnt signaling pathway, was detected by RT-qPCR in RAW264.7 cells, during treatment with (A) LIPUS and LPS or (B) LIPUS and IL4. RAW indicates RAW264.7 cells used as control. RAW-LPS indicates RAW264.7 cells treated with 100 ng/mL LPS to induce macrophage-like M1 polarization. RAW+LPS+LIPUS indicates RAW264.7 cells treated with 100 ng/mL LPS and low-intensity pulsed ultrasound. RAW+LIPUS indicates RAW264.7 cells treated with low-intensity pulsed ultrasound. RAW+IL4 indicates RAW264.7 cells treated with 20 ng/mL IL4 to induce macrophage-like M2 polarization. RAW+IL4+LIPUS indicates RAW264.7 cells treated with 20 ng/mL IL4 and low-intensity pulsed ultrasound. \* $P < 0.05$ , \*\* $P < 0.005$ , \*\*\*\* $P < 0.0001$ .

Full-size DOI: 10.7717/peerj.18448/fig-4

### The inhibitory effect of low-intensity pulsed ultrasound on the M1 polarization of RAW264.7 cells is dependent on the Wnt2b/AXIN/ $\beta$ -catenin pathway

Since Wnt2b was regulated by LIPUS and played roles in the inhibition of M1 polarization by LIPUS, the study next explored how LIPUS regulated the downstream proteins of Wnt2b, including AXIN and  $\beta$ -catenin. The expression of Wnt2b was knocked down by siRNA. The downregulation of Wnt2b (Fig. 6A) resulted in decreased expression of  $\beta$ -catenin (Fig. 6B) and increased expression of AXIN (Fig. 6C). These results indicated that the inhibition of M1 polarization of RAW264.7 cells by LIPUS is dependent on the Wnt2b/AXIN/ $\beta$ -catenin pathway.

### Downregulation of Wnt2b reversed the inhibitory effect of low-intensity pulsed ultrasound on the expression of inflammatory factors IL6 and TNF $\alpha$ in M1 polarization of RAW264.7 cells

To study the variation of inflammatory factors in LIPUS-treated and M1-polarized RAW264.7 cells, the cell culture supernatant was collected. Inflammatory factors IL2, IL4, IL6, IL10, TNF $\alpha$ , IFN $\gamma$ , and IL17A were detected by flow cytometry (Fig. 7A). The results showed that LIPUS inhibited the expression of IL6 and TNF $\alpha$  during LPS induction of RAW264.7 cells, while the downregulation of Wnt2b increased the expression of IL6 and TNF $\alpha$ . There was no significant change in the expression of IL2, IL4, IL10, IFN $\gamma$ , and

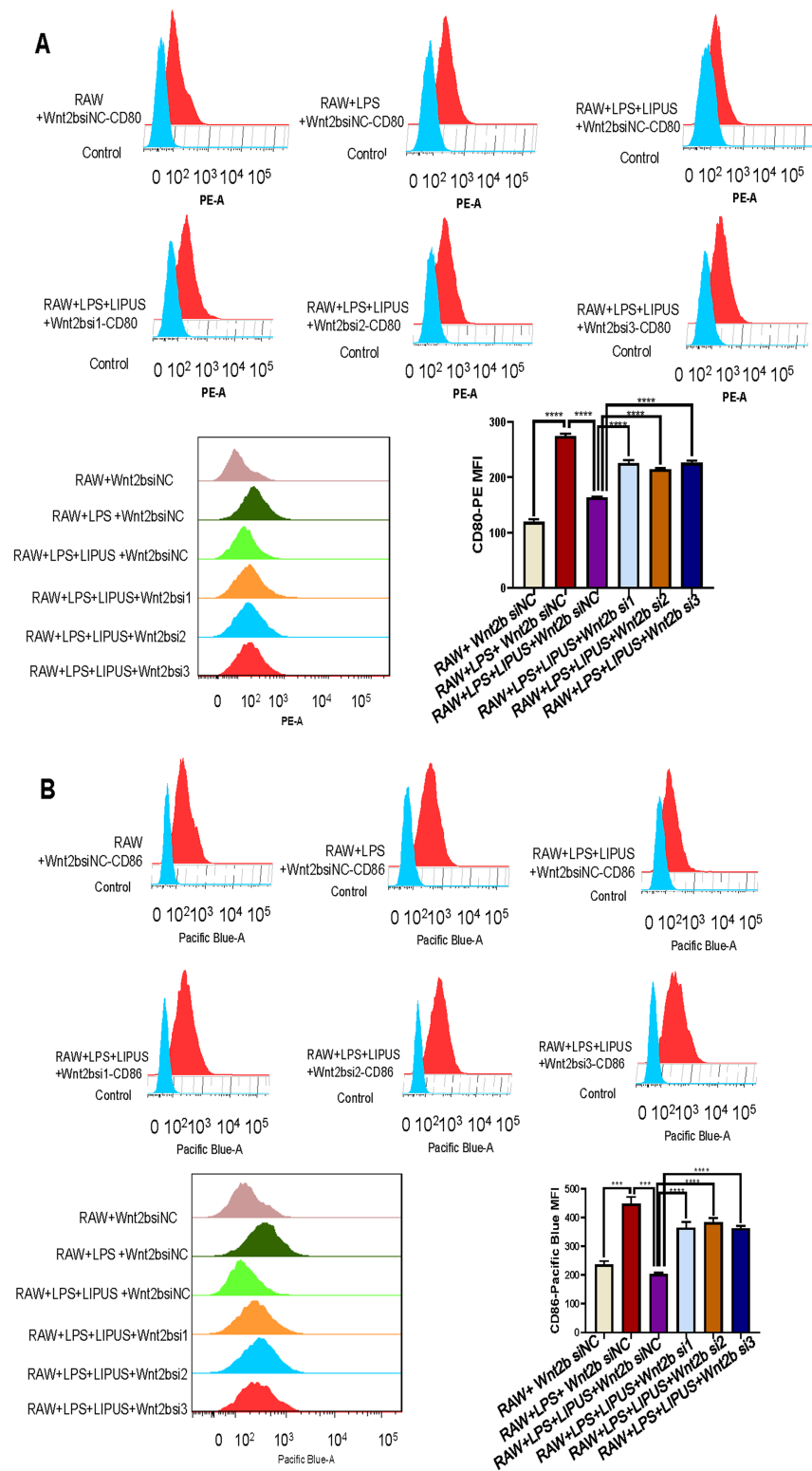


**Figure 5** Knocking down Wnt2b could reduce the inhibitory effect of low-intensity pulsed ultrasound on M1 polarization of RAW264.7 cells. (A) CD80 and (B) CD86 were detected by flow cytometry during M1 polarization of RAW264.7 cells. RAW+Wnt2bsiNC indicates RAW264.7 cells transfected with negative control of Wnt2b siRNA, used as control. RAW+LPS+Wnt2bsiNC indicates RAW264.7 cells transfected with negative control of Wnt2b siRNA and treated with 100 ng/mL LPS to

**Figure 5** (continued)

induce macrophage-like M1 polarization. RAW+LPS+LIPUS+Wnt2bsiNC indicates RAW264.7 cells transfected with negative control of Wnt2b siRNA and treated with 100 ng/mL LPS and low-intensity pulsed ultrasound. RAW+LPS+LIPUS+Wnt2bsi1/2/3 indicates RAW264.7 cells transfected with Wnt2b siRNA and treated with low-intensity pulsed ultrasound. \*\*\* $P < 0.0005$ , \*\*\*\* $P < 0.0001$ .

Full-size  DOI: [10.7717/peerj.18448/fig-5](https://doi.org/10.7717/peerj.18448/fig-5)

IL17A (Fig. 7B), suggesting that LIPUS inhibits the expression of IL6 and TNF $\alpha$  in a Wnt2b-dependent way.

## DISCUSSION

LIPUS has been used for decades as an adjuvant treatment for periodontitis. The biological mechanisms of LIPUS have been explored in multiple clinical models. One previous study found that LIPUS promoted osteogenesis of human periodontal ligament cells (hPDLs) and inhibited the periodontal inflammatory response by regulating the expression of TLR5 (Li *et al.*, 2024). Another study found that the combination of LIPUS and carboxymethyl cellulose significantly promoted cellular proliferation and osteoblast differentiation (Tang *et al.*, 2022). The enhancement of bone-tendon interface healing by LIPUS has been shown to be mediated by promoting the M2 polarization of macrophages (Li *et al.*, 2021b; Qin *et al.*, 2023; Zhang *et al.*, 2019). LIPUS significantly shifts macrophage phenotypes from M1 to M2, but the specific mechanism of LIPUS in inflammation and polarization of macrophages is not yet known. The results of the present study suggest that LIPUS inhibits the M1 polarization and promotes the M2 polarization of RAW264.7 cells. Wnt2b was found to be upregulated in the LIPUS-treated and LPS-induced RAW264.7 cells in polyA mRNA sequencing. The results also showed that LIPUS inhibits the M1 polarization of RAW264.7 cells in a Wnt2b/AXIN/ $\beta$ -catenin-dependent way. Downregulation of Wnt2b reversed the inhibitory effect of LIPUS on the expression of inflammatory factors IL6 and TNF $\alpha$  in the M1 polarization of RAW264.7 cells.

The Wnt pathway has been shown to participate in the treatment of skeletal disorders by helping repair bone tissue (Han, Yang & Hwang, 2022; Marini *et al.*, 2023; Xu *et al.*, 2022). The Wnt/ $\beta$ -catenin signaling pathway has been shown to be involved in LIPUS-mediated osteogenesis (Hua *et al.*, 2022). Another study found that activating Wnt signaling could increase total macrophages and pro-inflammatory macrophages (Avery *et al.*, 2022). However, the mechanism of how LIPUS regulates macrophages through the Wnt signaling pathway has not been clear.

Wnt2b is an important protein in the Wnt family, which is characterized by a Wnt-core domain. The proteins of the Wnt family perform functions in a variety of developmental processes including regulating cell growth and differentiation. The present study found that LIPUS promoted the relative expression of Wnt2b and that knocking down Wnt2b could reverse the inhibitory effects of LIPUS on M1 polarization of RAW264.7 cells, which depended on AXIN/ $\beta$ -catenin. The activation of the Wnt/ $\beta$ -catenin signaling pathway by LIPUS has been reported in previously published studies, one of which found that Wnt1 and  $\beta$ -Catenin significantly increased after ultrasound irradiation on the hepatic

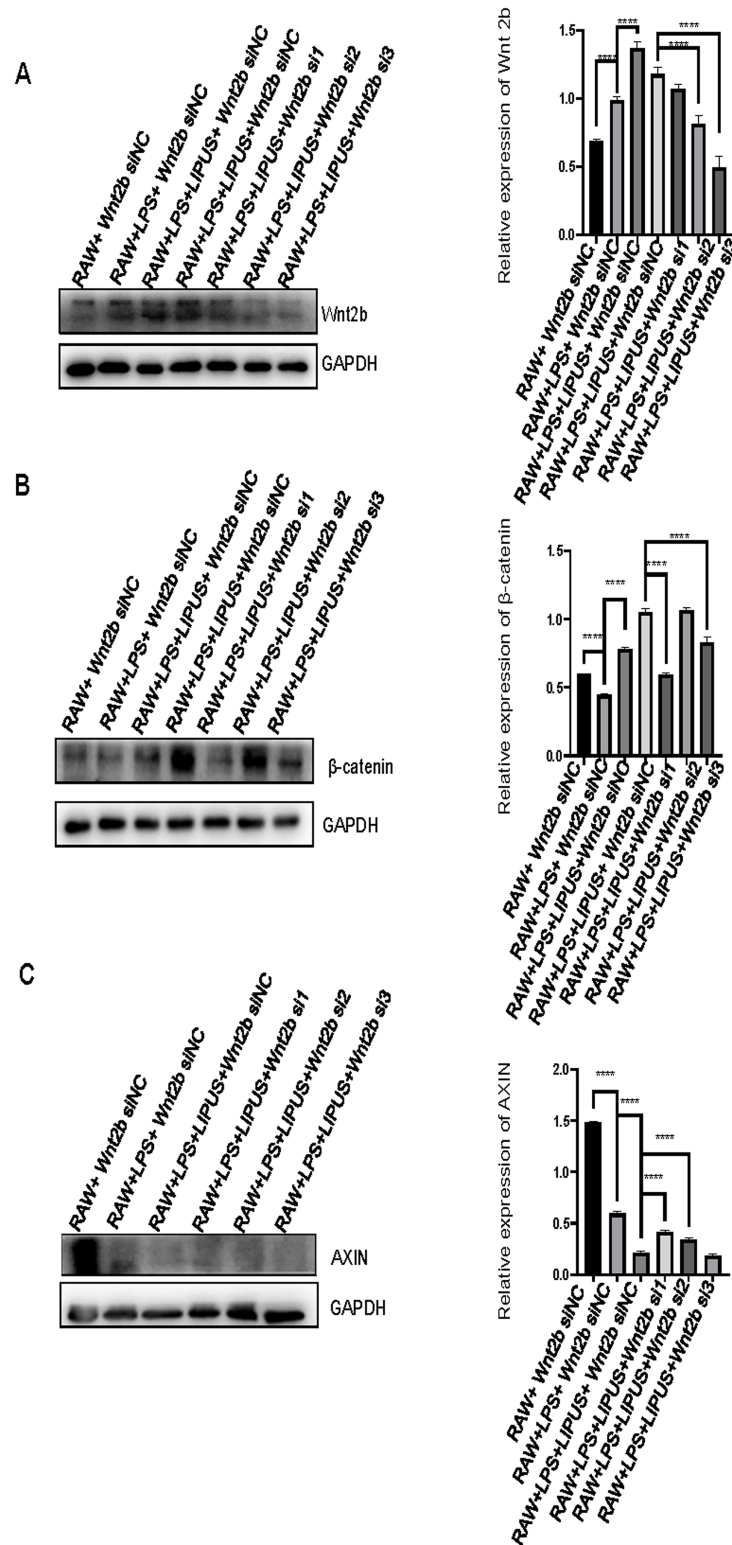


**Figure 6** Low-intensity pulsed ultrasound inhibited the M1 polarization of RAW264.7 cells in a Wnt2b/AXIN/β-catenin-dependent way. Relative expression of (A) Wnt2b, (B) AXIN, and (C) β-catenin detected by Western blot. RAW-Wnt2bsiNC indicates RAW264.7 cells transfected with negative control of Wnt2b siRNA, used as control. RAW+LPS+Wnt2bsiNC indicates RAW264.7 cells transfected with negative control of Wnt2b siRNA and treated with 100 ng/mL LPS to induce macrophage-like M1

**Figure 6** (continued)

polarization. RAW+LPS+LIPUS+Wnt2bsiNC indicates RAW264.7 cells transfected with negative control of Wnt2b siRNA and treated with 100 ng/mL LPS and low-intensity pulsed ultrasound. RAW+LPS+LIPUS+Wnt2bsi1/2/3 indicates RAW264.7 cells transfected with Wnt2b siRNA and treated with 100 ng/mL LPS and low-intensity pulsed ultrasound. \*\*\*\* $P < 0.0001$ . [Full-size !\[\]\(d84e7ea36f695d92cb39ec32c307ac93\_img.jpg\) DOI: 10.7717/peerj.18448/fig-6](https://doi.org/10.7717/peerj.18448/fig-6)

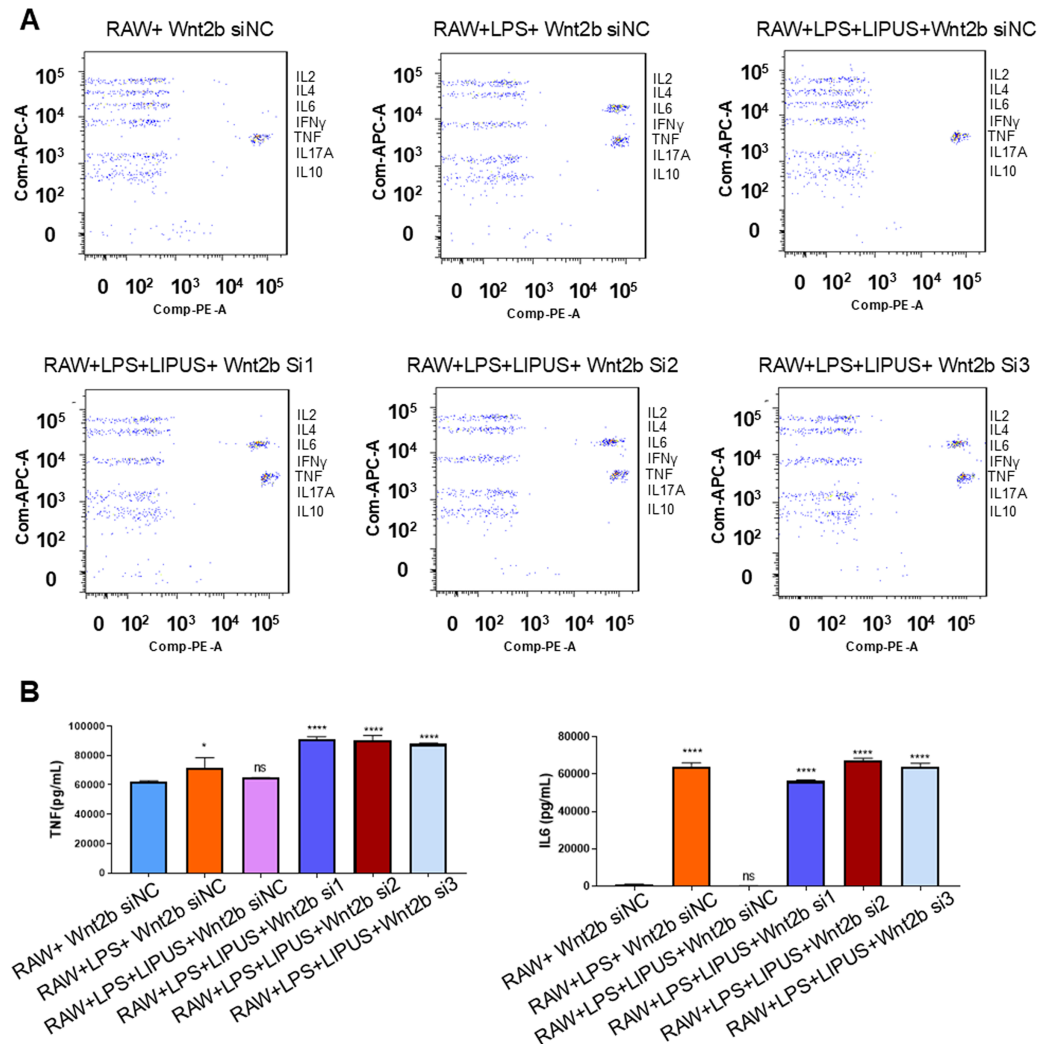


**Figure 7** Downregulation of Wnt2b reduced the effect of low-intensity pulsed ultrasound on inhibiting the expression of inflammatory factors IL6 and TNF $\alpha$  in M1 polarization of RAW264.7 cells. (A) The expression of IL2, IL4, IL6, IL10, TNF $\alpha$ , IFN $\gamma$ , and IL17A were detected by flow cytometry. (B) The expression of IL6 and TNF $\alpha$  was increased by the downregulation of Wnt2b during LIPUS and LPS treatment. RAW+Wnt2bsiNC indicates RAW264.7 cells transfected with negative control of Wnt2b siRNA, used as control. RAW+LPS+Wnt2bsiNC indicates RAW264.7 cells transfected with negative control of Wnt2b siRNA and treated with 100 ng/mL LPS to induce macrophage-like M1 polarization. RAW+LPS+LIPUS+Wnt2bsiNC indicates RAW264.7 cells transfected with negative control of Wnt2b siRNA and treated with 100 ng/mL LPS and low-intensity pulsed ultrasound. RAW+LPS+LIPUS+Wnt2bsi1/2/3 indicates RAW264.7 cells transfected with Wnt2b siRNA and treated with 100 ng/mL LPS and low-intensity pulsed ultrasound. \* $P < 0.05$ , \*\*\*\* $P < 0.0001$ .

[Full-size !\[\]\(83f22ed94ec5517769dd76d702c6bfd8\_img.jpg\) DOI: 10.7717/peerj.18448/fig-7](https://doi.org/10.7717/peerj.18448/fig-7)

differentiation of human bone marrow mesenchymal stem cells (Li et al., 2018). Whereas, in other studies, LIPUS has been reported to inhibit the Hh/Wnt pathway, which reversed the stem cell-related characteristics of cancer stem cells in one study (Song et al., 2022). Studies on the effect of LIPUS on the macrophage have found the Wnt pathway is activated by enhancing  $\beta$ -catenin nuclear translocation and upregulating frizzled class receptor 5 (FZD5) expression, resulting in M2-shifted macrophage polarization (Li et al., 2021b; Qin et al., 2023). In the present study, LIPUS inhibited the M1 polarization of RAW264.7 cells in a Wnt2b/AXIN/ $\beta$ -catenin-dependent way. These results provide a new perspective on the mechanism of LIPUS on macrophage M1 polarization.

The transmission of Wnt signaling plays important roles in tooth development and related oral diseases including periodontitis, cleft palate, jaw disease, dental pulp disease, and abnormal tooth development (Zhang et al., 2022). The Wnt signaling pathway is regulated by  $\beta$ -catenin. The ligands of the complex of frizzled (FZD) and low-density lipoprotein receptor-related proteins 5 and 6 (LRP5/6) receptors include Wnt1, Wnt2, Wnt3a, Wnt3b, Wnt8, and Wnt10b (Zhang et al., 2022). When the Wnt ligands bind to their receptors, the  $\beta$ -catenin complex is activated.  $\beta$ -catenin is transported to the nucleus and binds with TCF/LEF, leading to the expression of downstream target proteins, such as C-myc and CyclinD1 (Hayat, Manzoor & Hussain, 2022; Zhang et al., 2022). In the cytoplasm,  $\beta$ -catenin is phosphorylated by the complex of Axin, APC, and GSK-3 $\beta$ , resulting in the ubiquitination of  $\beta$ -catenin by the protease system (Rim, Clevers & Nusse, 2022; Zhang et al., 2022). Therefore, the regulation of the Wnt2b/AXIN/ $\beta$ -catenin pathway on macrophage polarization by LIPUS may play an important role in the treatment of periodontal disease.

This study found that LIPUS plays an anti-inflammatory role by inhibiting the LPS-induced M1 polarization of RAW264.7 cells in a Wnt2b/AXIN/ $\beta$ -catenin pathway-dependent way. However, there are limitations to this study. First, only *in vitro* experiments were carried out in this study. *In vivo*, studies using animal models of mice or rats should be performed to confirm the specific functions and mechanisms of LIPUS in the clinical treatment of periodontal diseases through the Wnt2b/AXIN/ $\beta$ -catenin pathway. Second, in-depth studies should be performed to explore how LIPUS affects the expression of Wnt2b/AXIN/ $\beta$ -catenin. Third, future in-depth studies should explore the effects and mechanism of LIPUS on the M2 polarization of RAW264.7 cells.

## CONCLUSIONS

LIPUS inhibited the expression of inflammatory cytokines and inhibited the LPS-induced M1 polarization of RAW264.7 cells in a Wnt2b/AXIN/ $\beta$ -catenin dependent way. LIPUS may play a role in inhibiting inflammation in periodontal diseases by regulating macrophage differentiation.

## ACKNOWLEDGEMENTS

The authors thank Meifen Li and Sai Ma for laboratory management.



## ADDITIONAL INFORMATION AND DECLARATIONS

### Funding

This work was supported by the Program of Jiangsu Science and Technology Department (BK20211083, BE2022737), the Program of Suzhou Health Commission (GSWS2020078, SZXK202111), the Program of Suzhou Science and Technology Department (SKY2023062, SKJY2021123). The funders had no role in study design, data collection and analysis, decision to publish, or preparation of the manuscript.

### Grant Disclosures

The following grant information was disclosed by the authors:

Program of Jiangsu Science and Technology Department: BK20211083, BE2022737.

Program of Suzhou Health Commission: GSWS2020078, SZXK202111.

Program of Suzhou Science and Technology Department: SKY2023062, SKJY2021123.

### Competing Interests

The authors declare that they have no competing interests.

### Author Contributions

- Juan Yin conceived and designed the experiments, performed the experiments, analyzed the data, prepared figures and/or tables, authored or reviewed drafts of the article, and approved the final draft.
- Yu Bao performed the experiments, analyzed the data, prepared figures and/or tables, and approved the final draft.
- Minxin Xu performed the experiments, analyzed the data, prepared figures and/or tables, authored or reviewed drafts of the article, and approved the final draft.
- Ping Li performed the experiments, prepared figures and/or tables, and approved the final draft.
- Zhipeng Zhang analyzed the data, prepared figures and/or tables, and approved the final draft.
- Hui Xue conceived and designed the experiments, authored or reviewed drafts of the article, and approved the final draft.
- Xing Yang conceived and designed the experiments, analyzed the data, authored or reviewed drafts of the article, and approved the final draft.

### DNA Deposition

The following information was supplied regarding the deposition of DNA sequences:

The RNA sequencing data is available at NCBI GEO: [GSE273466](https://www.ncbi.nlm.nih.gov/geo/query/acc.cgi?acc=GSE273466).

### Data Availability

The following information was supplied regarding data availability:

Raw data are available as a [Supplemental File](#).

Flow cytometry data are available in the FlowRepository database: FR-FCM-Z7KP.

<http://flowrepository.org/id/RvFrC3z0IIg1UDM1mrwEIIgYgNzSiAq40h3r7E4kS4Lorl1mQgTICkwsq8XU6b7D>

## Supplemental Information

Supplemental information for this article can be found online at <http://dx.doi.org/10.7717/peerj.18448#supplemental-information>.

## REFERENCES

- Abaricia JO, Shah AH, Chaubal M, Hotchkiss KM, Olivares-Navarrete R. 2020.** Wnt signaling modulates macrophage polarization and is regulated by biomaterial surface properties. *Biomaterials* **243**:119920 DOI [10.1016/j.biomaterials.2020.119920](https://doi.org/10.1016/j.biomaterials.2020.119920).
- Avery D, Morandini L, Sheakley LS, Shah AH, Bui L, Abaricia JO, Olivares-Navarrete R. 2022.** Canonical Wnt signaling enhances pro-inflammatory response to titanium by macrophages. *Biomaterials* **289**:121797 DOI [10.1016/j.biomaterials.2022.121797](https://doi.org/10.1016/j.biomaterials.2022.121797).
- Bao J, Yang Y, Xia M, Sun W, Chen L. 2021.** Wnt signaling: an attractive target for periodontitis treatment. *Biomedicine & Pharmacotherapy* **133(2013)**:110935 DOI [10.1016/j.biopha.2020.110935](https://doi.org/10.1016/j.biopha.2020.110935).
- Bertolini M, Clark D. 2024.** Periodontal disease as a model to study chronic inflammation in aging. *Geroscience* **46(4)**:3695–3709 DOI [10.1007/s11357-023-00835-0](https://doi.org/10.1007/s11357-023-00835-0).
- Guan X, He Y, Wei Z, Shi C, Li Y, Zhao R, Pan L, Han Y, Hou T, Yang J. 2021.** Crosstalk between Wnt/ $\beta$ -catenin signaling and NF- $\kappa$ B signaling contributes to apical periodontitis. *International Immunopharmacology* **98(12)**:107843 DOI [10.1016/j.intimp.2021.107843](https://doi.org/10.1016/j.intimp.2021.107843).
- Hajishengallis G. 2022.** Interconnection of periodontal disease and comorbidities: evidence, mechanisms, and implications. *Periodontology 2000* **89(1)**:9–18 DOI [10.1111/prd.12430](https://doi.org/10.1111/prd.12430).
- Han JJ, Yang HJ, Hwang SJ. 2022.** Enhanced bone regeneration by bone morphogenetic Protein-2 after pretreatment with low-intensity pulsed ultrasound in distraction osteogenesis. *Tissue Engineering and Regenerative Medicine* **19(4)**:871–886 DOI [10.1007/s13770-022-00457-1](https://doi.org/10.1007/s13770-022-00457-1).
- Hayat R, Manzoor M, Hussain A. 2022.** Wnt signaling pathway: a comprehensive review. *Cell Biology International* **46(6)**:863–877 DOI [10.1002/cbin.11797](https://doi.org/10.1002/cbin.11797).
- Hua Z, Li S, Liu Q, Yu M, Liao M, Zhang H, Xiang X, Wu Q. 2022.** Low-intensity pulsed ultrasound promotes osteogenic potential of iPSC-derived MSCs but fails to simplify the iPSC-EB-MSC differentiation process. *Frontiers in Bioengineering and Biotechnology* **10**:841778 DOI [10.3389/fbioe.2022.841778](https://doi.org/10.3389/fbioe.2022.841778).
- Jiang Y, Han Q, Zhao H, Zhang J. 2021.** Promotion of epithelial-mesenchymal transformation by hepatocellular carcinoma-educated macrophages through Wnt2b/ $\beta$ -catenin/c-Myc signaling and reprogramming glycolysis. *Journal of Experimental & Clinical Cancer Research* **40**:13 DOI [10.1186/s13046-020-01808-3](https://doi.org/10.1186/s13046-020-01808-3).
- Jiang X, Savchenko O, Li Y, Qi S, Yang T, Zhang W, Chen J. 2019.** A review of low-intensity pulsed ultrasound for therapeutic applications. *IEEE Transactions on Biomedical Engineering* **66(10)**:2704–2718 DOI [10.1109/TBME.2018.2889669](https://doi.org/10.1109/TBME.2018.2889669).
- Li H, Deng Y, Tan M, Feng G, Kuang Y, Li J, Song J. 2020a.** Low-intensity pulsed ultrasound upregulates osteogenesis under inflammatory conditions in periodontal ligament stem cells through unfolded protein response. *Stem Cell Research & Therapy* **11**:215 DOI [10.1186/s13287-020-01732-5](https://doi.org/10.1186/s13287-020-01732-5).
- Li F, Liu Y, Cai Y, Li X, Bai M, Sun T, Du L. 2018.** Ultrasound irradiation combined with hepatocyte growth factor accelerate the hepatic differentiation of human bone marrow

- mesenchymal stem cells. *Ultrasound in Medicine & Biology* **44**(5):1044–1052  
DOI [10.1016/j.ultrasmedbio.2018.01.005](https://doi.org/10.1016/j.ultrasmedbio.2018.01.005).
- Li Y, Sun C, Feng G, He Y, Li J, Song J. 2020b.** Low-intensity pulsed ultrasound activates autophagy in periodontal ligament cells in the presence or absence of lipopolysaccharide. *Archives of Oral Biology* **117**(2):104769 DOI [10.1016/j.archoralbio.2020.104769](https://doi.org/10.1016/j.archoralbio.2020.104769).
- Li S, Xu Z, Wang Z, Xiang J, Zhang T, Lu H. 2021b.** Acceleration of bone-tendon interface healing by low-intensity pulsed ultrasound is mediated by macrophages. *Physical Therapy* **101**(7):520 DOI [10.1093/ptj/pzab055](https://doi.org/10.1093/ptj/pzab055).
- Li P, Zhang Z, Liu J, Xue H. 2024.** LIPUS can promote osteogenesis of hPDLs and inhibit the periodontal inflammatory response via TLR5. *Oral Diseases* **30**(5):3386–3399  
DOI [10.1111/odi.14807](https://doi.org/10.1111/odi.14807).
- Li X, Zhong Y, Zhou W, Song Y, Li W, Jin Q, Gao T, Zhang L, Xie M. 2023.** Low-intensity pulsed ultrasound (LIPUS) enhances the anti-inflammatory effects of bone marrow mesenchymal stem cells (BMSCs)-derived extracellular vesicles. *Cellular & Molecular Biology Letters* **28**:9  
DOI [10.1186/s11658-023-00422-3](https://doi.org/10.1186/s11658-023-00422-3).
- Li H, Zhou J, Zhu M, Ying S, Li L, Chen D, Li J, Song J. 2021a.** Low-intensity pulsed ultrasound promotes the formation of periodontal ligament stem cell sheets and ectopic periodontal tissue regeneration. *Journal of Biomedical Materials Research Part A* **109**(7):1101–1112  
DOI [10.1002/jbm.a.37102](https://doi.org/10.1002/jbm.a.37102).
- Liang C, Yang T, Wu G, Li J, Geng W. 2020.** The optimal regimen for the treatment of temporomandibular joint injury using low-intensity pulsed ultrasound in rats with chronic sleep deprivation. *BioMed Research International* **2020**:5468173 DOI [10.1155/2020/5468173](https://doi.org/10.1155/2020/5468173).
- Liu J, Xiao Q, Xiao J, Niu C, Li Y, Zhang X, Zhou Z, Shu G, Yin G. 2022.** Wnt/ $\beta$ -catenin signalling: function, biological mechanisms, and therapeutic opportunities. *Signal Transduction and Targeted Therapy* **7**:3 DOI [10.1038/s41392-021-00762-6](https://doi.org/10.1038/s41392-021-00762-6).
- Majnooni M, Lasaygues P, Long V, Scimeca JC, Momier D, Rico F, Buzhinsky N, Guivier-Curien C, Baron C. 2022.** Monitoring of in-vitro ultrasonic stimulation of cells by numerical modeling. *Ultrasonics* **124**(8):106714 DOI [10.1016/j.ultras.2022.106714](https://doi.org/10.1016/j.ultras.2022.106714).
- Marini F, Giusti F, Palmi G, Brandi ML. 2023.** Role of Wnt signaling and sclerostin in bone and as therapeutic targets in skeletal disorders. *Osteoporosis International* **34**(2):213–238  
DOI [10.1007/s00198-022-06523-7](https://doi.org/10.1007/s00198-022-06523-7).
- Naruse H, Itoh S, Itoh Y, Kagioka T, Abe M, Hayashi M. 2021.** The Wnt/ $\beta$ -catenin signaling pathway has a healing ability for periapical periodontitis. *Scientific Reports* **11**(1):19673  
DOI [10.1038/s41598-021-99231-x](https://doi.org/10.1038/s41598-021-99231-x).
- Palanisamy P, Alam M, Li S, Chow SKH, Zheng YP. 2022.** Low-intensity pulsed ultrasound stimulation for bone fractures healing: a review. *Journal of Ultrasound in Medicine* **41**(3):547–563 DOI [10.1002/jum.15738](https://doi.org/10.1002/jum.15738).
- Pamuk F, Kantarci A. 2022.** Inflammation as a link between periodontal disease and obesity. *Periodontology 2000* **90**(1):186–196 DOI [10.1111/prd.12457](https://doi.org/10.1111/prd.12457).
- Qin H, Luo Z, Sun Y, He Z, Qi B, Chen Y, Wang J, Li C, Lin W, Han Z, Zhu Y. 2023.** Low-intensity pulsed ultrasound promotes skeletal muscle regeneration via modulating the inflammatory immune microenvironment. *International Journal of Biological Sciences* **19**(4):1123–1145 DOI [10.7150/ijbs.79685](https://doi.org/10.7150/ijbs.79685).
- Rim EY, Clevers H, Nusse R. 2022.** The Wnt pathway: from signaling mechanisms to synthetic modulators. *Annual Review of Biochemistry* **91**:571–598  
DOI [10.1146/annurev-biochem-040320-103615](https://doi.org/10.1146/annurev-biochem-040320-103615).

- Seasons GM, Pellow C, Kuipers HF, Pike GB. 2024. Ultrasound and neuroinflammation: immune modulation via the heat shock response. *Theranostics* **14**(8):3150–3177 DOI [10.7150/thno.96270](https://doi.org/10.7150/thno.96270).
- Song S, Ma D, Xu L, Wang Q, Liu L, Tong X, Yan H. 2022. Low-intensity pulsed ultrasound-generated singlet oxygen induces telomere damage leading to glioma stem cell awakening from quiescence. *iScience* **25**(1):103558 DOI [10.1016/j.isci.2021.103558](https://doi.org/10.1016/j.isci.2021.103558).
- Sumitomo R, Huang CL, Ando H, Ishida T, Cho H, Date H. 2022. Wnt2b and Wnt5a expression is highly associated with M2 TAMs in non-small cell lung cancer. *Oncology Reports* **48**(5):7 DOI [10.3892/or.2022.8404](https://doi.org/10.3892/or.2022.8404).
- Tang L, Wu T, Zhou Y, Zhong Y, Sun L, Guo J, Fan X, Ta D. 2022. Study on synergistic effects of carboxymethyl cellulose and LIPUS for bone tissue engineering. *Carbohydrate Polymers* **286**:119278 DOI [10.1016/j.carbpol.2022.119278](https://doi.org/10.1016/j.carbpol.2022.119278).
- Tian X, Wu Y, Yang Y, Wang J, Niu M, Gao S, Qin T, Bao D. 2020. Long noncoding RNA LINC00662 promotes M2 macrophage polarization and hepatocellular carcinoma progression via activating Wnt/ $\beta$ -catenin signaling. *Molecular Oncology* **14**(2):462–483 DOI [10.1002/1878-0261.12606](https://doi.org/10.1002/1878-0261.12606).
- Wang Y, Li J, Qiu Y, Hu B, Chen J, Fu T, Zhou P, Song J. 2018a. Low-intensity pulsed ultrasound promotes periodontal ligament stem cell migration through TWIST1-mediated SDF-1 expression. *International Journal of Molecular Medicine* **42**:322–330 DOI [10.3892/ijmm.2018.3592](https://doi.org/10.3892/ijmm.2018.3592).
- Wang Y, Qiu Y, Li J, Zhao C, Song J. 2018b. Low-intensity pulsed ultrasound promotes alveolar bone regeneration in a periodontal injury model. *Ultrasonics* **90**:166–172 DOI [10.1016/j.ultras.2018.06.015](https://doi.org/10.1016/j.ultras.2018.06.015).
- Wang Y, Xiao Q, Zhong W, Zhang C, Yin Y, Gao X, Song J. 2022. Low-intensity pulsed ultrasound promotes periodontal regeneration in a beagle model of furcation involvement. *Frontiers in Bioengineering and Biotechnology* **10**:961898 DOI [10.3389/fbioe.2022.961898](https://doi.org/10.3389/fbioe.2022.961898).
- Weinstock A, Rahman K, Yaacov O, Nishi H, Menon P, Nikain CA, Garabedian ML, Pena S, Akbar N, Sansbury BE, Heffron SP, Liu J, Marecki G, Fernandez D, Brown EJ, Ruggles KV, Ramsey SA, Giannarelli C, Spite M, Choudhury RP, Loke P, Fisher EA. 2021. Wnt signaling enhances macrophage responses to IL-4 and promotes resolution of atherosclerosis. *Elife* **10**:100 DOI [10.7554/eLife.67932](https://doi.org/10.7554/eLife.67932).
- Wu H, Dong H, Tang Z, Chen Y, Liu Y, Wang M, Wei X, Wang N, Bao S, Yu D, Wu Z, Yang Z, Li X, Guo Z, Shi L. 2023. Electrical stimulation of piezoelectric BaTiO<sub>3</sub> coated Ti6Al4V scaffolds promotes anti-inflammatory polarization of macrophages and bone repair via MAPK/JNK inhibition and OXPHOS activation. *Biomaterials* **293**(9):121990 DOI [10.1016/j.biomaterials.2022.121990](https://doi.org/10.1016/j.biomaterials.2022.121990).
- Wu T, Zheng F, Tang HY, Li HZ, Cui XY, Ding S, Liu D, Li CY, Jiang JH, Yang RL. 2024. Low-intensity pulsed ultrasound reduces alveolar bone resorption during orthodontic treatment via Lamin A/C-Yes-associated protein axis in stem cells. *World Journal of Stem Cells* **16**(3):267–286 DOI [10.4252/wjsc.v16.i3.267](https://doi.org/10.4252/wjsc.v16.i3.267).
- Xu Z, Li S, Wan L, Hu J, Lu H, Zhang T. 2022. Role of low-intensity pulsed ultrasound in regulating macrophage polarization to accelerate tendon-bone interface repair. *Journal of Orthopaedic Research* **41**:919–929 DOI [10.1002/jor.25454](https://doi.org/10.1002/jor.25454).
- Yin J, Ye YL, Hu T, Xu LJ, Zhang LP, Ji RN, Li P, Chen Q, Zhu JY, Pang Z. 2020. Hsa\_circRNA\_102610 upregulation in Crohn's disease promotes transforming growth factor- $\beta$ 1-induced epithelial-mesenchymal transition via sponging of hsa-miR-130a-3p. *World Journal of Gastroenterology* **26**(22):3034–3055 DOI [10.3748/wjg.v26.i22.3034](https://doi.org/10.3748/wjg.v26.i22.3034).

- Zhang Z, Pan X, Chen M, Bai M. 2022.** Wnt signalling in oral and maxillofacial diseases. *Cell Biology International* **46(1)**:34–45 DOI [10.1002/cbin.11708](https://doi.org/10.1002/cbin.11708).
- Zhang ZC, Yang YL, Li B, Hu XC, Xu S, Wang F, Li M, Zhou XY, Wei XZ. 2019.** Low-intensity pulsed ultrasound promotes spinal fusion by regulating macrophage polarization. *Biomedicine & Pharmacotherapy* **120(12)**:109499 DOI [10.1016/j.biopha.2019.109499](https://doi.org/10.1016/j.biopha.2019.109499).
- Zhou LN, Bi CS, Gao LN, An Y, Chen F, Chen FM. 2019.** Macrophage polarization in human gingival tissue in response to periodontal disease. *Oral Diseases* **25(1)**:265–273 DOI [10.1111/odi.12983](https://doi.org/10.1111/odi.12983).